

# Modelling of Microspring Thermal Actuator

J.K.Luo, A.J.Flewitt, S.M.Spearing\*, N.A.Fleck and W.I.Milne

Eng. Dept. Cambridge University, Trumpington Street, Cambridge, CB2 1ZP U.K.

\*Dept. of Aeronautics & Astronautics, MIT, Cambridge, MA, 02139, USA

## Abstract

A new type of Microspring ( $\mu$ -spring) electrothermal actuator consisting of multi-chevron structures was proposed. Finite element analysis was used to model the device performance, and the results compared with that of chevron thermal actuator. The simulation showed that the  $\mu$ -spring actuator can deliver a much large deflection than that of chevron actuator. The deflection is proportional to the number of chevron structures linked together. By linking more chevron structures, this  $\mu$ -spring can deliver a larger displacement than any other thermal actuators. The device has a much smaller footage than that of a single chevron device for a similar amount of deflection. Electroplated Ni thin film and SiO<sub>2</sub> were used as active and linkage materials to fabricate the  $\mu$ -spring actuator.

**Keyword:** electrothermal actuator, microspring actuator, chevron, metal MEMS.

## 1. Introduction

Microelectrothermal actuators are one of the most attractive micro-moving actuators as they can deliver large forces and displacements compared to other types of actuators such as piezoelectric and electrostatic actuators. Electro-thermal actuators that utilises the difference in thermal expansion coefficient between two layers of a bilayer structure for vertical actuation (out of the plane of the layer) and others that utilises different structures made from the same material to induce varying expansions and motion in-plane have been reported previously [1,2]. The latter is preferential as it is a planar structure, suitable for the integration, especially on the CMOS. In order to obtain a large displacement and force for this type of flexure devices, a number of thermal actuators are typically connected in series [3]. Chevron type actuators [4], as shown in **Fig.1 a**, provide an even larger displacement, but such a single beam like device is difficult to integrate into a system. Here we report the development of a new type of planar microspring ( $\mu$ -spring) thermal actuator. Finite element analysis (FEA) is used to simulate the device performance, and electroplated Ni thin film was used to fabricate the device.

## 2. Device concept and modelling

The deflection of a chevron actuator strongly depends on the length and the angle of the beams; a larger deflection is produced if a smaller angle is used. The drawback is that it is a single beam like device. To deliver a larger displacement, even longer beams are required for chevron actuators. This is problematical in term of fabrication and operation, as the long beams easily buckle or stick to the substrate. Therefore the beam length of a chevron device is limited, typically to a 200 $\mu$ m long, which in-turn limits the amount of the displacement and applications. In our new type of device, instead of using a single long beam, the arm is folded into a number of chevron sections to become a planar spring-like actuator as shown in **Fig.1.b**. (2 chevrons with 1 linkage bar are defined as 1 ring). An insulating beam with a very low thermal expansion coefficient is used to form a cross-linkage thereby constraining the displacement in the x-direction. As the actuator is heated up under bias, the thermal expansion of the active material leads to a displacement in the y-direction only.

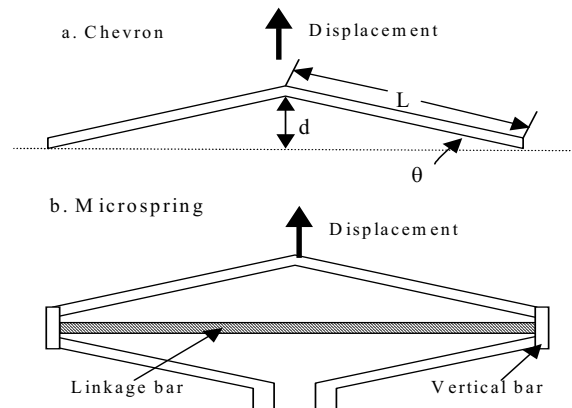


Figure.1 Schematic drawing of a).chevron and b).  $\mu$ -spring actuators with 1 ring.

For a chevron device, the displacement in y direction under bias can be estimated as follows [4].

$$\Delta y \approx \frac{L\Delta L}{d} \approx \frac{\Delta L}{\sin \theta} \approx \frac{\alpha L \Delta T}{\theta} \quad (1)$$

Here  $\alpha$  is the thermal expansion coefficient of the beam material; d the height of a chevron device and L is the

beam length. Assuming the convection and the radiation make little contribution to the heat loss, then the temperature distribution along the beams is governed by the classic heat transfer equation [1,4,5],

$$k \frac{d^2 T}{dx^2} + J^2 \rho = 0 \quad (2)$$

$$J = \frac{V}{RA} = \frac{V}{\rho L} \quad (3)$$

Where  $J$  is the current density,  $V$  the applied voltage,  $L$  the length of the resistor,  $R$  the resistance,  $A$  the cross section of the beam,  $\rho$  the resistivity and  $k$  the thermal conductivity. The maximum temperature is at the joint point of two beams, and the average temperature  $\Delta T_{ave}$  of the beam is given by:

$$\Delta T_{ave} = \int \frac{T(x) - T_o}{2L} dx = \frac{V^2}{3k\rho} = \frac{PL}{3kA} \quad (4)$$

where  $P = IV$  the consumed power. The deflection can be expressed as follows,

$$\Delta y \approx \beta \frac{\alpha L \Delta T_{ave}}{\theta} = \beta \frac{\alpha L V^2}{3k\rho\theta} = \beta \frac{\alpha P L^2}{3kA\theta} \quad (5)$$

where  $\beta$  is the coefficient,  $\beta = 1$  for chevron device and  $\beta < 1$  for spring actuator as will be discussed later. At a small angle,  $\theta \approx d/L$ , eq.(5) then becomes,

$$\Delta y \approx \beta \frac{\alpha L^2 V^2}{3k\rho d} = \beta \frac{\alpha P L^3}{3kAd} \quad (6)$$

At a fixed bias  $V$  and material properties, the deflection is proportional to the square of the beam length, while for a fixed power  $P$ , the deflection increases with the cubic of the beam length; therefore increasing the beam length is the most effective way to achieve a larger displacement. As mentioned above, there is a limitation to the beam length due to buckling and stiction problems, the maximum displacement of a chevron actuator is therefore limited. Reducing the height  $d$  of the structure has the similar effects to increase the risk of buckling and stiction as increasing the beam length. Therefore increasing the beam length and reducing the height is not the best way to improve the device performance. On the other hand, by introducing a multi-chevron spring structure, the buckling and stiction issues can be solved readily, as the folded beams reduce the length in one direction.

The deflection of a  $\mu$ -spring actuator is similar to that of a chevron device and the displacement in  $y$ -direction can also be expressed by eqs.(5) and (6) with a modified coefficient  $\beta$ , as the current does not pass through the insulator. The main contributions to a modified coefficient  $\beta$  are from the limited thermal expansion of the insulator

beam at an elevated temperature, which leads to a displacement in  $x$ -direction, and reduce the displacement in  $y$ -direction. Also introduction of vertical bars to link beams together causes a slight deflection in  $x$ -direction. When the heat loss through the surface is considered, then the linkage bars lose more heat owing to increased surface area. Therefore the coefficient  $\beta$  for a  $\mu$ -spring actuator is always smaller than 1, as we will see later from FEA modelling.

From eq.(6), it is understood that active materials with a higher value of  $\alpha/k$  are better for thermal actuators. Metals generally provide a larger displacement than Si based materials as most metals have a much larger thermal expansion coefficient [5]. Insulator such as  $\text{SiN}_x$  and  $\text{SiO}_2$  are among the best materials for cross linkage bars, as they have the lowest thermal expansion coefficients. Nickel and silicon nitride were chosen as the materials for beams and cross-linkage bars respectively for the simulation. Thermal radiation and convection are neglected here as they only contribute a few percent to the total heat loss in the temperature range of interest. Finite element analysis based on the FEMLAB software was used to simulate the performance of both chevron and  $\mu$ spring actuators. In the simulation, the temperature dependence of the resistivity was considered, and the voltage operation mode was used instead of the current operation mode. The constants used for this simulation are listed in Table.I, where the resistivity, its temperature coefficient and the Young's modulus for Ni thin films were obtained experimentally from our work [5].

**Table.I**

	$\alpha \cdot 10^{-6}$ (/C°)	$\rho$ ( $\Omega \cdot \text{cm}$ )	$\kappa$ (W/M.°C)	E (GPa)	$\xi \cdot 10^{-3}$ (/°C)
Ni	12.7	$2 \times 10^{-7}$	83	210	~3.0
$\text{SiN}_x$	2.0	n/a	20	~150	n/a
$\text{SiO}_2$	0.4	n/a	2	~150	n/a

### 3. Microfabrication

Microspring actuators were fabricated using a two-mask process, and the process flow is shown in Fig.2. The first mask stage is the formation of the insulator cross-linkage bars. Stress free LPCVD  $\text{Si}_3\text{N}_4$  or thermally grown  $\text{SiO}_2$  were used as the linkage bars. Photoresist patterns were used as an etch mask to etch  $\text{Si}_3\text{N}_4$  or  $\text{SiO}_2$  with concentrated HF or BHF. After the formation of linkage bars, a seed layer of Cr/Cu (10/50nm) was deposited on the wafer by sputtering. Positive photoresist AZ5214 was used to form the plating mould. A multilayer coating method was used to form a thick mould with a thickness of  $\sim 3\mu\text{m}$  [5]. Stress free Ni thin films were then electroplated using nickel sulphamate solution at an optimised conditions of  $60^\circ\text{C}$  and  $2 \sim 4\text{mA}/\text{cm}^2$  current density. The typical thickness of actuator devices is  $1.5 \sim 2\mu\text{m}$ . After plating, the photoresist

and the seed layer out side of device area were removed by acetone and acid respectively, and was followed by releasing process. For  $\text{Si}_3\text{N}_4$  linkage bars, the actuators were released by a wet etching in a KOH (20% in wt) solution at  $85^\circ\text{C}$  for  $\sim 30$ mins, while for the  $\text{SiO}_2$  bars, the devices were released by SF6 RIE dry etching as SF6 has a good etch selectivity between Si and  $\text{SiO}_2$ . More detailed description of the process can be found in Ref.5.

It was found that the adhesion between the Cr/Cu seed layer and the  $\text{Si}_3\text{N}_4$  bar is very poor, and it detaches from each other at various process stages. Some special treatments can improve the adhesion, but the yield of successful devices was very low. On the other hand, the adhesion between the  $\text{SiO}_2$  and the Cr/Cu seed layer is excellent; there is no delamination problem.

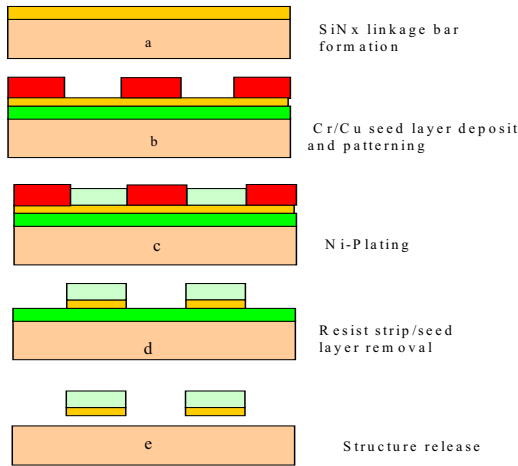


Fig.2 Process flow for fabricating actuators.

#### 4. Results and discussions

**Figure 3** shows the simulated displacement and the temperature distribution for a microspring actuator with 2-rings of chevron structures under a bias of 0.4V. The beam length and width are 200 and  $4\mu\text{m}$  respectively. The angle is  $d/L=0.1$ . The maximum temperature is at the top of the middle point,  $T_{\text{max}}=923\text{K}$ , the displacement is  $33.7\mu\text{m}$ . The displacement of the lower chevron is small because of a lower temperature, while that for the upper chevron is large owing to a higher temperature. For a steady state, the linkage bar has a similar temperature to that of the joint points with the arms, and the temperature is uniform along the bar. The temperature distribution along the beams for a  $\mu$ -spring was found to be similar to that of a chevron actuator, with a parabolic distribution. But there are temperature dips at the joint points of the beams and the linkage bars due to the heat loss through the linkage bars. For dynamic state, it was found that the temperature of a linkage bar is not uniform, and the temperature at the middle of the bar is lower than that on the edge owing to a finite time constant for the heat transfer.

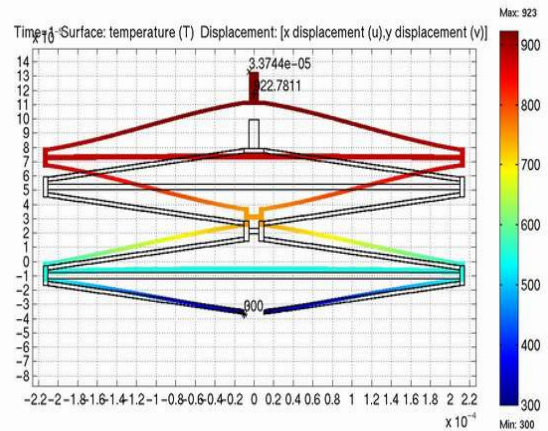


Figure 3 the temperature and displacement distribution of a 2-rings  $\mu$ spring at a bias of 0.4V. It delivers a deflection of  $\sim 34\mu\text{m}$  with  $T_{\text{max}}$  of 923K.

Simulation was also performed for chevron actuator devices with the same beam length and cross-section. The angle for chevrons is also set  $d/L=0.1$ . The deflection results are shown in **Fig.4** together with those of spring actuators with the total beam length as a variable, at a fixed bias of 0.4V. The displacement for a chevron device increases linearly with increasing the beam length as predicted by the analytical eq.(5). For a chevron actuator with  $L=200\mu\text{m}$ , will deliver a displacement of  $10.2\mu\text{m}$ . By introducing another chevron structure to form a 1-ring spring actuator with the same beam length  $200\mu\text{m}$  (total length is  $400\mu\text{m}$ ), it delivers a displacement of  $16.7\mu\text{m}$ , much larger than that of a chevron actuator. The displacement of a  $\mu$ -spring increases with increasing the number of chevron structures connected in series. When 2-rings chevron structures are used to form a spring, it can produce a displacement up to  $33.4\mu\text{m}$ . For this amount of displacement, a chevron actuator device with  $L=600\mu\text{m}$  is needed, which is not a desirable size for fabrication and operation. From the point of device area, this large chevron device occupies an area of  $2 \times 600 \times 60\mu\text{m}^2$ , while the corresponding 2-rings spring actuator only takes an area of  $\sim 220 \times 20 \times 2 \times 4\mu\text{m}^2$ , less than half the area of the chevron actuator. By connecting more chevron structures together, e.g. 6-rings, a spring actuator can produce a displacement as much as  $\sim 100\mu\text{m}$ , much larger than any planar actuators can produce. This has clearly showed the advantage of a  $\mu$ -spring actuator over any other actuators.

**Fig.4** also showed the dependence of the displacement of a spring actuator with  $L=100\mu\text{m}$  on the total beam length for comparison with that of  $L=200\mu\text{m}$ . It is clear that there exists a difference in displacement between the spring and the chevron actuators. The coefficient  $\beta$  decreases from chevron's  $\beta=1$  to  $\beta=0.81$  and  $\beta=0.71$  for spring actuators with  $L=200$  and  $L=100\mu\text{m}$  respectively. A smaller  $\beta$  for  $L=100\mu\text{m}$  springs is because more linkage and vertical bars are used. This result also indicates it is possible to

maximize the device performance by optimizing the device structure with a  $\beta$  close to 1. From the FEA simulation it was found that the deflection and the maximum temperature increase with increasing the square of the bias, consistent with the analytical results shown by eqs.(4) and (6).

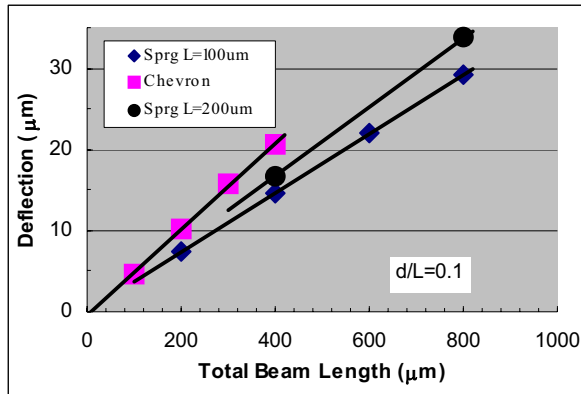


Fig.4 The deflection of chevron and spring actuators as a function of total beam length. The deflection of spring actuator increases with increasing the number of chevron connected.

Microsprings with varying beam lengths and the number of rings were fabricated. The beam lengths for chevron structures were 100, 200 and 400µm, while the ring numbers were 1, 2, 4 and 6. The length of vertical bars was 20µm. The width of the insulator bar was typically 4~6µm, while the beam width 3~4µm. At the tip of the actuator, a bar with multi-scales was also designed for measuring the deflection. It was found that with a Ni film thinner than 0.8µm, the beams easily buckle under the bias, a thicker Ni metal is therefore required for a proper operation of a µ-spring device.

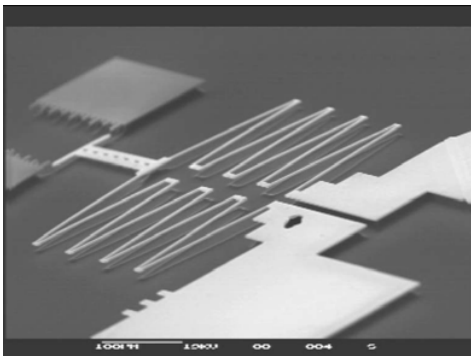


Fig.5 SEM picture of spring actuator without insulator linkage bars. Plating Ni was used, and released by SF6 dry etch.

**Figure 5** shows a SEM micrograph of a fabricated µ-spring without insulator cross-linkages. The structure has 4-rings with the beam length of 200µm, and was released

by SF6 dry etch. The electroplated Ni structure is freestanding with no visible curvature, indicating the gradient stress is at its minimum. The total length of the spring arms on one side is 800µm.

**Figure 6** shows a micrograph of a µ-spring with oxide constraint bars. The oxide thickness is ~1.0µm. These insulator bars hold the beams tightly without separating from the Ni-beams. Preliminary electrical test showed a motion of µ-spring along y-direction, and the displacement increases with increasing the ring number.

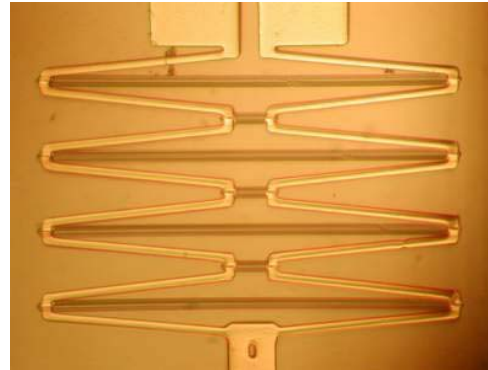


Fig.6 micrograph of a 4-rings spring actuator with SiO<sub>2</sub> (dark) linkage bars. L=200µm.

## 5. Conclusions

A new spring type of electrothermal actuator has been proposed and modelled by FEA. This spring type actuator delivers a much larger deflection than all other electrothermal actuators, but with a much-reduced device area. This type of device minimizes the buckling and stiction problem, which are associated with long beam devices, thus it is easy to integrate with the system. Spring actuator has been fabricated using electroplated Ni as active material and electrically tested.

**Acknowledgement:** This project was sponsored by the Cambridge-MIT Institute under grant number 059/P

## References

1. Q.A.Huang and N.K.S.Lee, *J. Micromech. MicroEng.* **9**, 64 (1999).
2. L.Que, J.S.Park and Y.B.Gianchandani; *J.Microelectro. mech.sys.* **10**, 247 (01')
3. J.R.Reid, V.M.Bright and J.H.Comtois *Proc. of SPIE* **96 2882**, 296 (1996).
4. R.Hichey, D.Sameoto, T.Hubbard and M.Kujath; *J. Micromech. MicroEng.* **13**, 40 (2003).
5. J.K.Luo, J.H.He, A.J.Flewitt, S.M.Spearing, N.A.Fleck and W.I.Milne; *Proc. of SPIE 04 Conf.* In press.
6. W.N.Jr.Sharpe, "Mechanical Properties of MEMS Materials" 2001, Johns Hopkins University: Baltimore, MD USA